Non-cell autonomous Otx2 homeoprotein regulates visual cortex plasticity through Gadd45b

Jessica Apulei[1,2], Namsuk Kim[1,2], Damien Testa[1,2], Jérôme Ribot[1], Clémence Bernard[1], Ariel A. Di Nardo[1]*, Alain Prochiantz[1]

[1]Centre for Interdisciplinary Research in Biology (CIRB), Collège de France, CNRS UMR 7241/INSERM U1050, PSL University, Labex memolife, Paris, France

[2]Co-first author (alphabetical order)

Correspondence: ariel.dinardo@college-de-france.fr (A.A.D.)

Tel: +33 1 44 27 14 56; Fax: +33 1 44 27 15 65

Running title: Cortical Otx2 targets Gadd45b

Abstract

The non-cell autonomous transfer of Otx2 homeoprotein transcription factor into juvenile mouse cerebral cortex regulates parvalbumin interneuron maturation and critical period timing. By analyzing gene expression in primary visual cortex of wild-type and *Otx2*$^{+/GFP}$ mice at plastic and non-plastic ages, we identified several putative genes implicated in Otx2-dependent visual cortex plasticity for ocular dominance. We find that Otx2 transfer regulates *Gadd45b/g* expression, which can potentially modify the epigenetic state of parvalbumin interneurons as evidenced by changes in MeCP2 foci size and number. Blocking Otx2 transfer in the adult, which induces plasticity, resulted in *Gadd45b/g* upregulation and changes in MeCP2 foci. Viral expression of

Gadd45b in adult visual cortex directly induced plasticity with concomitant changes in MeCP2 foci. This interaction provides a molecular mechanism for Otx2 to promote critical period plasticity yet suppress adult plasticity.

Keywords: critical period, ocular dominance, parvalbumin interneuron, epigenetics, optical imaging

Introduction

Experience-dependent plasticity shapes neural circuits in postnatal life during defined transient windows of heightened plasticity, or critical periods (CP), which generally begin in primary sensory areas and move up to more integrated brain regions, ending with plasticity in cortices involved with higher cognition. The developmental importance of such plasticity is exemplified by the loss of visual acuity following monocular deprivation (MD) during the CP for ocular dominance (OD). Imbalanced visual input reduces visual acuity of the "lazy eye" during infancy and leads to amblyopia, which afflicts 2-5% of the human population (Holmes and Clarke 2006). After CP closure, intrinsic potential for plasticity is actively dampened in order to stabilize brain circuits (Takesian and Hensch 2013).

Critical periods are influenced by the non-cell autonomous transfer of Otx2 homeoprotein transcription factor, which controls the maturation of GABAergic fast-spiking parvalbumin interneurons (PV cells) and is required in adult mice for the maintenance of a non-plastic state (Sugiyama et al. 2008; Beurdeley et al. 2012; Spatazza et al. 2013; Bernard et al. 2016). The Otx2 homeoprotein possesses conserved sequence features within the homeodomain that permit translocation between cells (Joliot et al. 1991). In the brain, Otx2 is secreted by the choroid plexus, transported to the cortex, and then internalized by PV cells enwrapped by extracellular perineuronal nets (PNN) (Beurdeley et al. 2012; Spatazza et al. 2013; Kim et al. 2014). Therefore, non-cell autonomous Otx2 has access to the entire cortex and can indeed control the timing of multiple CPs (Lee et al. 2017). Importantly, Otx2 begins to accumulate prior to CP onset and continues to accumulate after CP closure. Thus, Otx2-regulated plasticity can be explained by a two-threshold model for increased Otx2 accumulation in PV cells: a first concentration threshold triggers CP

onset while crossing a second threshold induces and maintains CP closure (Prochiantz and Di Nardo 2015). Furthermore, Otx2 is attracted by the PNNs that specifically enwrap PV cells, thus permitting a constant accumulation of Otx2 in certain PV cells throughout the cortex (Bernard and Prochiantz 2016). However, the molecular mechanisms that allow Otx2 to promote cortex plasticity in juvenile mice yet suppress plasticity in adult mice, have not been elucidated.

Epigenetic changes are also implicated in cortical plasticity, as CP is regulated by chromatin reorganization through DNA methylation and histone modifications (Putignano et al. 2007; Krishnan et al. 2015; Lennartsson et al. 2015; Nott et al. 2015; Tognini et al. 2015; Krishnan et al. 2017). DNA methylation can repress transcription by blocking DNA binding of transcription factors or by recruiting repressor complexes containing histone deacetylase to condense chromatin structures (Fagiolini et al. 2009). Here, we identify *Gadd45b* as a direct target of Otx2 in visual cortex. Gadd45b-dependent DNA demethylation has been implicated in neurogenesis, long-term memory and genomic stability (Hollander et al. 1999; Rai et al. 2008; Leach et al. 2012; Niehrs and Schäfer 2012). We provide molecular evidence that Otx2 regulates *Gadd45b* expression in either direction, which permits Otx2 to stimulate CP plasticity yet dampen adult plasticity.

Materials and Methods

Ethics statement

All animal procedures were carried out in accordance with the guidelines of the European Economic Community (2010/63/UE) and the French National Committee (2013/118). For surgical procedures, animals were anesthetized with Xylazine

(Rompun 2%, 5 mg/kg) and Ketamine (Imalgene 1000, 80 mg/kg). This project (no. 00704.02) obtained approval from Ethics committee n° 59 of the French Ministry for Research and Higher Education.

Animals

Conventionally raised C57Bl/6N mice were purchased from Janvier Laboratories. *Otx2*$^{+/GFP}$ knock-in mice were kindly provided by Drs. D. Acampora and A. Simeone (IGB, Naples, Italy). The *scFvOtx2*$^{tg/o}$ and *scFvPax6*$^{tg/o}$ mouse lines were generated through a knock-in approach, as described previously (Bernard et al. 2016).

Brain injections and infusions

Stereotaxic injections into visual cortex (lambda: x = 1.7 mm, y = 0 mm, z = 0.5 mm) of 300 ng of his-Otx2 protein (Beurdeley et al. 2012) or vehicle (0.9% NaCl), with or without 0.1 µg/µl cycloheximide (Sigma) in 2 µl were performed with Hamilton syringe at 0.2 µl/min. For conditional choroid plexus expression, intracerebroventricular stereotaxic injections (bregma: x = -0.58 mm, y = ±1.28 mm, z = 2 mm) of 40 µg of Cre-TAT protein (Spatazza et al. 2013) in 15% DMSO, 1.8% NaCl in 4 µl were performed with a Hamilton syringe at 0.2 µl/min. Two weeks after injection, mice were processed for layer IV dissection as previously described (Bernard et al. 2016). For adeno-associated virus (AAV) infection, 2 µl (3.4 x 10^{11} GC/ml) of either AAV8-Syn-mCherry-2A-mGadd45b (Vector BioLabs) or AAV8-Syn-mCherry (Vector BioLabs) were injected in visual cortex as described above. Two weeks after injection, mice were processed for layer IV dissection, histology or monocular deprivation.

Stereotaxic infusions into visual cortex (above coordinates) with 3 d osmotic mini pump (Alzet 1003D, Charles River Laboratories) were used to deliver 100 µl of either cycloheximide (0.1 µg/µl, Sigma) and/or actinomycin D (0.2 µg/µl, Sigma) in 0.9% NaCl.

RNA sequencing

Visual cortex layer IV dissected from 4 mice were pooled for each sample, prior to RNA extraction by RNeasy Mini Kit (Qiagen). Duplicate samples were treated with DNase I and sent to the IBENS Genomics Facility (Ecole Normale Supérieure, Paris) for library construction and Illumina sequencing. Data processing and analysis was performed by the Genomics Facility. The accession number for this data is GEO: GSE98258.

Quantitative RT-PCR

Total RNA was extracted from dissected tissue by using the AllPrep DNA/RNA Mini Kit (Qiagen). cDNA was synthesized from 200 ng of total RNA with QuantiTect Reverse Transcription kit (Qiagen). Quantitative PCR reactions were carried out in triplicate with SYBR Green I Master Mix (Roche) on a LightCycler 480 system (Roche). Expression was calculated by using the $2^{-\Delta\Delta Ct}$ method with Gapdh as a reference.

In situ hybridization

In situ hybridization was performed as previously described (Di Nardo et al., 2007). Briefly, cryosections (20 µm) were hybridized overnight at 70°C with a digoxigenin (DIG)-labeled RNA probe for *Gadd45b/g* mRNA. After washing, sections were incubated with alkaline phosphatase-conjugated anti-DIG (1/2000; Roche) overnight at 4°C. DAB staining (Vector Laboratories) was carried out according to manufacturer's instructions.

Immunohistochemistry

Mice were perfused transcardially with PBS followed by 4% paraformaldehyde prepared in PBS. Brains were post-fixed 1 h at 4°C and immunohistochemistry was performed on cryosections (20 µm) encompassing the entire visual cortex. Heat-induced antigen retrieval by 10 mM sodium citrate was performed only for anti-MeCP2 experiments prior to overnight 1° antibody incubation at 4°C. Primary antibodies included anti-MeCP2 (rabbit, 1/200, Millipore), anti-mCherry (mouse, 1/200, Clontech), anti-parvalbumin (rabbit, 1/200, SWANT), biotinylated WFA (1/100, Sigma), and anti-Gapdh (rabbit, 1/250, abcam). Secondary antibodies were Alexa Fluor-conjugated (Molecular Probes). Images were acquired with a Leica SP5 confocal microscope and analyzed with ImageJ.

Monocular deprivation and surgery for optical imaging

For monocular deprivation, mice were anesthetized prior to suturing of the left eye as previously described (Gordon and Stryker 1996). Animals were checked daily to ensure sutures remained intact. The eye was opened immediately before recording.

For optical imaging, mice were anesthetized with urethane (1.2 g/kg, i.p.) and sedated with chlorprothixene (8 mg/kg, i.m.). Atropine (0.1 mg/kg) and dexamethasone (2 mg/kg) were injected subcutaneously with body temperature maintained at 37°C.

Visual stimulation and optical imaging recording

Visual cortical responses were recorded using imaging methods based on Fourier transform following periodic stimulation (Kalatsky and Stryker 2003; Cang et al. 2005). A high refresh rate monitor was placed 20 cm in front of stereotaxically restrained mouse. Stimulation consisted of a horizontal bar drifting downwards periodically at 1/8 Hz in the binocular visual field of the recorded hemisphere (from +5° ipsilateral to +15° contralateral). Each eye was stimulated 5 times alternately for 4 minutes. Intrinsic signals were recorded using a 1M60 CCD camera (Dalsa) with a 135x50 mm tandem lens (Nikon) configuration. After acquisition of the surface vascular pattern, the focus of the camera was lowered by 400 μm deeper. Intrinsic signals were acquired with a 700 nm illumination wavelength and frames stored at a rate of 10 Hz, after a 2x2 pixels spatial binning.

Data analysis

Functional maps for each eye were calculated offline. Prior to Fourier transform, slow varying components independent of the stimulation were subtracted by the generalized indicator function (Yokoo et al. 2001). Retinotopic organization and intensity were computed from the phase and magnitude components of the signal at the frequency of stimulation. For each eye, the five activity maps were averaged, filtered with a Gaussian kernel low-pass filter (3 pixels s.d.) and set with a cut-off

threshold at 50% of the maximum response. The binocular zone was defined as the intersection between the response regions of each eye. For each session, an OD value at each pixel was defined as (C-I)/(C+I), calculated from the response amplitude from the contralateral (C) eye and the ipsilateral (I) eyes. The OD index was then computed for each session as the average of the OD values in the binocular zone. Consequently, OD index ranged from -1 to 1, with negative values representing an ipsilateral bias, and positive values a contralateral bias.

Statistical analysis

Statistical analysis was performed with Prism 6 (GraphPad). Pairwise comparison was performed with Student t-test, while multiple group analyses were done with ANOVA (one- or two-way) followed by Bonferroni correction.

Results

Non-cell autonomous regulation of gene expression by Otx2 in the visual cortex

A better understanding of how Otx2 regulates plasticity in the visual cortex requires that its non-cell autonomous transcription targets be identified. We dissected layer IV of the visual cortex and used RNA-sequencing to analyze gene expression at postnatal day 30 (P30) and P100 in wild-type (WT) mice, and at P30 in the *Otx2*$^{+/GFP}$ heterozygotes. The rationale is that CP plasticity is opened at P30 in WT but not in *Otx2*$^{+/GFP}$ mice, given that *Otx2* genetic deletion delays CP opening (Sugiyama et al. 2008), and that the CP is closed at P100 in WT mice. Thus, genes with similar expression at P30 in *Otx2*$^{+/GFP}$ and at P100 in WT mice but with a different level of

expression at P30 in WT mice were considered as potential genes involved in plasticity. After applying a threshold cut-off of 2-fold change in expression between P30 and P100 in WT mice, we identified 20 candidate genes, all of them up-regulated during CP (Fig. 1A). This small list contains several immediate early genes, including *Arc*, *Fos*, *Egr1/2/4* and *Nr4a*, already implicated in cerebral cortex plasticity (Kaczmarek and Chaudhuri 1997; Andreasson and Kaufmann 2002; Li et al. 2005; Shepherd and Bear 2011; Vallès et al. 2011; Tognini et al. 2015; Bernard et al. 2016).

However, while this approach revealed potential "plasticity genes" within layer IV, it does not identify genes directly regulated by non-cell autonomous Otx2 in PV cells. In the mouse visual cortex, CP for binocular vision opens at P20 once internalized Otx2 has reached a first concentration threshold (Spatazza et al. 2013). We reasoned that direct Otx2 transcriptional targets are not dependent on protein synthesis (do not require an intermediate target) and thus that their transcripts might still be up-regulated in the presence of cycloheximide (CHX), a blocking agent for protein translation. Low-dose CHX, or vehicle, was infused in the visual cortex between P20 and P23 and the efficiency of the drug was verified by the decreased expression of Gapdh, a protein with a short half-life (Fig. 1B) (Mansur et al. 1993). Upon CHX infusion, only *Gadd45b/g*, and *Pvr* were still significantly up-regulated (Fig. 1C), suggesting that the transcription of all the other candidate genes between P20 and P23 was either not direct or required translation of a co-factor. Because CHX has been reported to stabilize some transcripts (Ooi et al. 1993), we verified whether the up-regulation of these three genes is indeed transcription-dependent by co-infusion of CHX and actinomycin D, a transcription inhibitor. This cocktail eliminated *Pvr* (Fig. 1C), suggesting that *Gadd45b/g* are the best candidates for direct regulation by Otx2.

To confirm direct *Gadd45b/g* regulation by non–cell autonomous Otx2, we injected recombinant his-Otx2 protein at P17 with or without CHX. Cortical injection or infusion of Otx2 protein result in specific uptake by PV cells (Sugiyama et al. 2008; Beurdeley et al. 2012) and anticipates CP opening (Sugiyama et al. 2008). Exogenous Otx2 increased the expression of *Gadd45b/g* and *Pvr* 6 hours after injection (Fig. 1D). This finding further suggests that *Gadd45b/g* are direct Otx2 targets in the sense that only Otx2 is necessary for their expression 6 hours after its internalization and that this increase is maintained in the presence of CHX, in contrast with that of *Pvr*. *Gadd45b/g* may therefore directly relay Otx2 activity to regulate plasticity in the visual cortex.

Before exploring this hypothesis further, we confirmed that *Gadd45b/g* cortical expression not only increases between P21 and P30, but also declines as plasticity is turned off (Fig. 1E) and that the two genes are expressed in the cells that internalize Otx2 (Fig. 1F). Extra-cortical Otx2 is primarily internalized by PV cells through their PNNs, which can be stained by the lectin *Wisteria Floribunda Agglutinin* (WFA). Both *Gadd45b/g* are expressed within WFA-stained neurons (Fig. 1F), even though the overlap is only 50% (Fig. 1G).

Gadd45b regulates the expression of plasticity genes in the mouse visual cortex

To further verify the correlation between Otx2 internalization and the expression of plasticity genes including *Gadd45b/g*, we took advantage of two conditional mouse lines carrying anti-Otx2 or anti-Pax6 single chain antibodies (scFv): *scFvOtx2*$^{tg/o}$ and *scFvPax6*$^{tg/o}$. The expression and secretion of these antibodies (scFv-Otx2 and scFv-Pax6) can be induced specifically in the adult choroid plexus by injecting a cell-

permeable Cre recombinase (Cre-TAT) in the lateral ventricles (Bernard et al. 2016). Secreted scFv-Otx2 neutralizes Otx2 in the cerebrospinal fluid (CSF), reduces the amount of Otx2 internalized by PV cells, induces a strong expression of *Arc*, *Fos*, *Egr4* and *Nr4a1* in layer III/IV of the visual cortex, and reopens of a period of physiological plasticity in the adult (Bernard et al. 2016). We now show that induction of scFv-Otx2 but not scFv-Pax6 increased *Gadd45b* and *Gadd45g* expression in the adult visual cortex (Fig. 2A). This finding reinforces the correlation between *Gadd45b/g* expression and plasticity, not only during juvenile development but also in the adult.

A consequence of *Gadd45b/g* being direct targets of Otx2, in contrast with *bona fide* "plasticity genes" (Fig. 1C), is that some of these genes may be controlled by *Gadd45b*. To verify this possibility, their expression was measured after low-titer viral expression of *Gadd45b* (AAV8-Syn-mCherry-2A-Gadd45b) in the visual cortex of adult (3-month-old) mice, which results in overexpression mainly in PV cells (Fig. 2B). Similar to what was observed during juvenile development (Fig. 1E) and after induced adult plasticity (Fig. 2A), *Gadd45b* expression was increased 2-fold on average, which resulted in up-regulation of *Gadd45g* and other "plasticity genes" including *Egr2*, *Arc*, *Fos* and *Egr4* (Fig. 2C). Furthermore, the expression level of these genes was directly correlated with that of *Gadd45b* (Fig. 2D), suggesting a proportional effect of *Gadd45b* expression on cortical plasticity.

Gadd45b gain of function reopens physiological plasticity in the adult visual cortex

The ability of Gadd45b to reactivate the expression of "plasticity genes" in the adult suggested that it may also reopen physiological plasticity. OD bias was measured by recording the retinotopic map with intrinsic optical imaging of binocular V1 after sequential activation of each eye. Adult mice injected with AAV8-Syn-mCherry control did not reopen physiological plasticity: after 4 d MD of the contralateral eye, mice had a similar OD to uninjected adult mice without MD (Fig. 3A,B,D,E). However, injection of AAV8-Syn-mCherry-2A-Gadd45b led to an OD shift (Fig. 3C-E). The reduction in OD index was mediated by a decrease of the deprived eye response (Fig. 3E). No change in the ipsilateral eye response was observed.

Gadd45b controls the methylation state of visual cortex

Given that Gadd45b has demethylase activity, we assessed the methylation state of visual cortex layer IV by evaluating the localization of Methyl CpG Binding Protein 2 (MeCP2), a marker for DNA methylation, at several different ages (P20, P30, P60, P100). Quantification of the number of MeCP2 foci revealed a decrease during postnatal development specifically in WFA-positive cells (Fig. 4A,B). The observed changes in expression of plasticity genes could happen through rearrangement of the chromatin structure towards a heterochromatic state, or by accumulation of MeCP2 protein on CpG islands within promoters of these genes. We observed the same intensity for MeCP2 protein staining but an increase in the area of foci in adult mice (Fig. 4C,D), suggesting a change in chromatin to a more compact state.

The reduction of MeCP2 foci specifically in V1 WFA-positive cells during postnatal development follows the kinetics of WFA intensity (Lee et al. 2017), suggesting it reflects a consolidated state of mature PV cells. While PNN assembly takes several

weeks to reach maximum, it remains surprisingly dynamic in adult V1 when Otx2 levels are reduced (Beurdeley et al. 2012; Spatazza et al. 2013; Bernard et al. 2016). We find MeCP2 foci show similar dynamics, as reopening adult plasticity by blocking Otx2 in CSF of *scFvOtx2*$^{tg/o}$ mice led to an increase of the number of MeCP2 foci in visual cortex WFA-positive PV cells compared to *scFvPax6*$^{tg/o}$ mice (Fig. 4E). This increase is similar to the number of foci observed in WT mice at the peak of plasticity (Fig. 4E). We also observed an increase in MeCP2 foci in visual cortex WFA-positive PV cells of adult mice injected with AAV8-Syn-mCherry-2A-Gadd45b compared to the mice injected with AAV8-Syn-mCherry (Fig. 4F). Thus, both Otx2 and Gadd45b levels in PV cells impact chromatin structure.

Discussion

The Gadd45 family has been implicated in epigenetic gene activation (Barreto et al. 2007; Ma et al. 2009; Gavin et al. 2012; Chen et al. 2016), which can impact synaptic plasticity, long-term memory and ultimately animal behavior (Leach et al. 2012; Sultan et al. 2012; Kigar et al. 2015). Furthermore, *Gadd45* genes have altered expression in mouse visual cortex after MD (Majdan and Shatz 2006; Tognini et al. 2015). Thus, changes in Gadd45b/g activity could have broad impact on gene regulation during PV cell maturation for CP timing. We find that when Otx2 protein levels are transiently increased in PV cells prior to CP onset, *Gadd45b/g* levels are rapidly increased in a translation-independent manner. Furthermore, when Gadd45b expression is increased in PV cells of adult cortex, we find juvenile-like MeCP2 foci along with increased layer IV plasticity gene expression and reactivated OD plasticity. This suggests that Otx2 signaling impacts PV cell maturation and function through

Gadd45b/g, which can control the expression of a swath of genes and leave epigenetic marks that would eventually stabilize during CP closure and be maintained into adulthood.

It is intriguing that Otx2 regulates Gadd45b/g oppositely in the juvenile and adult cortex. MeCP2 foci number and size gradually change in PV cells over the course of the CP and through to adulthood. In comparison, the state of MeCP2 foci in PV cells rapidly reverses when Otx2 signaling is compromised in adult, a paradigm that reactivates cortical plasticity (Bernard et al. 2016), suggesting that Otx2 impacts the epigenetic state of PV cells by regulating chromatin structure. Increasing levels of Otx2 may affect chromatin accessibility differently in juvenile and adult mice and subtly change PV cell activity. During brain development, homeoproteins have morphogenic activity that is critically dependent on concentration which allows the precise guidance of axons or the formation of regional boundaries (Prochiantz and Di Nardo 2015). Homeoproteins have also been implicated in DNA damage response and chromatin remodeling (Rekaik et al. 2015).

Thus, it is possible that Otx2-induced alterations in chromatin structure are proportional to the amount of non-cell autonomous Otx2 protein. To investigate this hypothesis, it will be necessary to compare the chromatin structure of PV cells before, during, and after the CP, and after inducing adult plasticity. Another non-exclusive possibility is that Otx2 interacts with other factors that may differ during the CP and post-CP. Such physiological interactions between homeoprotein signal transduction and classical signaling pathways has been demonstrated for Engrailed and Pax6 (Wizenmann et al. 2009; Di Lullo et al. 2011; Layalle et al. 2011; Stettler et al. 2012). This does not preclude that some genes are induced (or repressed) continuously by Otx2 activity in juvenile and adult such as PNN regulating genes (Lee et al. 2017).

Regardless, the change in epigenetic context between juvenile and adult PV cells, as revealed by MeCP2 foci, provides a compelling explanation for differential *Gadd45b/g* regulation by Otx2 activity. As *Gadd45b/g* are epigenetic modifiers (Niehrs and Schäfer 2012), their gradual decrease in expression from CP to adulthood may also be directly implicated in changing chromatin structure within PV cells.

The differential kinetics in MeCP2 foci number we observed during postnatal visual cortex development suggest differential recruitment in pyramidal cells and PV cells. Indeed, distinct phenotypes are observed in mice with either general or cell-specific removal of *MeCP2* expression. In *MeCP2-null* mice, PV cell maturation is premature and CP timing is also accelerated (Krishnan et al. 2015), which could be explained by the fact that MeCP2 normally represses brain-derived neutrophic factor expressed in pyramidal cells (Chen et al. 2003; Sampathkumar et al. 2016). Mice lacking MeCP2 only in excitatory neurons experience tremors and anxiety-like behaviors (Meng et al. 2016), whereas mice lacking MeCP2 only in PV cells do not show such phenotypes yet have completely abolished critical period plasticity (He et al. 2014). Clearly, MeCP2 recruitment is dependent on the type of neuron and likely its context, impacting a wide variety of mouse phenotypes (Gogolla et al. 2014; He et al. 2014; Krishnan et al. 2015; Meng et al. 2016; Sampathkumar et al. 2016). Reducing Otx2 activity in adult visual cortex directly impacted MeCP2 foci number in PNN-enwrapped cells, suggesting that Otx2 plays a role in differential MeCP2 recruitment. It will be important to determine the foci identity and the epigenetic fingerprint of PV cells, since it has been suggested that MeCP2 is implicated in cell-specific epigenetic mechanisms for regulation of gene expression and chromatin structure (Mellén et al. 2012).

While homeoproteins are well-characterized as transcription factors, they also actively control DNA replication and repair, mRNA export and translation, and protein degradation (Rezsohazy 2014; Prochiantz and Di Nardo 2015; Rezsohazy et al. 2015). As non-cell autonomous signaling factors, they have direct access to cytoplasm and nucleus with the potential to broadly impact function of the target cell. By regulating Gadd45b/g activity, Otx2 in PV cells could engage epigenetic programs that control the balance between plastic and non-plastic states.

Acknowledgments

This work was supported by the Fondation Bettencourt Schueller and by an ERC Advanced Grant (HOMEOSIGN, n° 339379 to A.P.).

References

Andreasson KI, Kaufmann WE. 2002. Role of immediate early gene expression in cortical morphogenesis and plasticity. Results Probl Cell Differ. 39:113–137.

Barreto G, Schäfer A, Marhold J, Stach D, Swaminathan SK, Handa V, Döderlein G, Maltry N, Wu W, Lyko F, Niehrs C. 2007. Gadd45a promotes epigenetic gene activation by repair-mediated DNA demethylation. Nature. 445:671–675.

Bernard C, Prochiantz A. 2016. Otx2-PNN Interaction to Regulate Cortical Plasticity. Neural Plast. 2016:1–7.

Bernard C, Vincent C, Testa D, Bertini E, Ribot J, Di Nardo AA, Volovitch M, Prochiantz A. 2016. A Mouse Model for Conditional Secretion of Specific Single-Chain Antibodies Provides Genetic Evidence for Regulation of Cortical Plasticity by a Non-cell Autonomous Homeoprotein Transcription Factor. PLoS

Genet. 12:e1006035.

Beurdeley M, Spatazza J, Lee HHC, Sugiyama S, Bernard C, Di Nardo AA, Hensch TK, Prochiantz A. 2012. Otx2 binding to perineuronal nets persistently regulates plasticity in the mature visual cortex. Journal of Neuroscience. 32:9429–9437.

Cang J, Kalatsky VA, Löwel S, Stryker MP. 2005. Optical imaging of the intrinsic signal as a measure of cortical plasticity in the mouse. Vis Neurosci. 22:685–691.

Chen K, Long Q, Wang T, Zhao D, Zhou Y, Qi J, Wu Y, Li S, Chen C, Zeng X, Yang J, Zhou Z, Qin W, Liu X, Li Y, Li Y, Huang X, Qin D, Chen J, Pan G, Schöler HR, Xu G, Liu X, Pei D. 2016. Gadd45a is a heterochromatin relaxer that enhances iPS cell generation. EMBO Rep. 17:1641–1656.

Chen WG, Chang Q, Lin Y, Meissner A, West AE, Griffith EC, Jaenisch R, Greenberg ME. 2003. Derepression of BDNF transcription involves calcium-dependent phosphorylation of MeCP2. Science. 302:885–889.

Di Lullo E, Haton C, Le Poupon C, Volovitch M, Joliot A, Thomas J-L, Prochiantz A. 2011. Paracrine Pax6 activity regulates oligodendrocyte precursor cell migration in the chick embryonic neural tube. Development. 138:4991–5001.

Fagiolini M, Jensen CL, Champagne FA. 2009. Epigenetic influences on brain development and plasticity. Curr Opin Neurobiol. 19:207–212.

Gavin DP, Sharma RP, Chase KA, Matrisciano F, Dong E, Guidotti A. 2012. Growth arrest and DNA-damage-inducible, beta (GADD45b)-mediated DNA demethylation in major psychosis. Neuropsychopharmacology. 37:531–542.

Gogolla N, Takesian AE, Feng G, Fagiolini M, Hensch TK. 2014. Sensory Integration in Mouse Insular Cortex Reflects GABA Circuit Maturation. Neuron. 83:894–905.

Gordon JA, Stryker MP. 1996. Experience-dependent plasticity of binocular responses in the primary visual cortex of the mouse. J Neurosci. 16:3274–3286.

He L-J, Liu N, Cheng T-L, Chen X-J, Li Y-D, Shu Y-S, Qiu Z-L, Zhang X-H. 2014. Conditional deletion of Mecp2 in parvalbumin-expressing GABAergic cells results in the absence of critical period plasticity. Nat Comms. 5:5036.

Hollander MC, Sheikh MS, Bulavin DV, Lundgren K, Augeri-Henmueller L, Shehee R, Molinaro TA, Kim KE, Tolosa E, Ashwell JD, Rosenberg MP, Zhan Q, Fernández-Salguero PM, Morgan WF, Deng CX, Fornace AJ. 1999. Genomic instability in Gadd45a-deficient mice. Nat Genet. 23:176–184.

Holmes JM, Clarke MP. 2006. Amblyopia. Lancet. 367:1343–1351.

Joliot AH, Triller A, Volovitch M, Pernelle C, Prochiantz A. 1991. alpha-2,8-Polysialic acid is the neuronal surface receptor of antennapedia homeobox peptide. New Biol. 3:1121–1134.

Kaczmarek L, Chaudhuri A. 1997. Sensory regulation of immediate-early gene expression in mammalian visual cortex: implications for functional mapping and neural plasticity. Brain Res Brain Res Rev. 23:237–256.

Kalatsky VA, Stryker MP. 2003. New paradigm for optical imaging: temporally encoded maps of intrinsic signal. Neuron. 38:529–545.

Kigar SL, Chang L, Auger AP. 2015. Gadd45b is an epigenetic regulator of juvenile social behavior and alters local pro-inflammatory cytokine production in the rodent amygdala. Brain Behav Immun. 46:60–69.

Kim N, Acampora D, Dingli F, Loew D, Simeone A, Prochiantz A, Di Nardo AA. 2014. Immunoprecipitation and mass spectrometry identify non-cell autonomous Otx2 homeoprotein in the granular and supragranular layers of mouse visual cortex. F1000Res. 3:178.

Krishnan K, Lau BYB, Ewall G, Huang ZJ, Shea SD. 2017. MECP2 regulates cortical plasticity underlying a learned behaviour in adult female mice. Nat Comms.

8:14077.

Krishnan K, Wang B-S, Lu J, Wang L, Maffei A, Cang J, Huang ZJ. 2015. MeCP2 regulates the timing of critical period plasticity that shapes functional connectivity in primary visual cortex. Proc Natl Acad Sci USA. 112:E4782–E4791.

Layalle S, Volovitch M, Mugat B, Bonneaud N, Parmentier M-L, Prochiantz A, Joliot A, Maschat F. 2011. Engrailed homeoprotein acts as a signaling molecule in the developing fly. Development. 138:2315–2323.

Leach PT, Poplawski SG, Kenney JW, Hoffman B, Liebermann DA, Abel T, Gould TJ. 2012. Gadd45b knockout mice exhibit selective deficits in hippocampus-dependent long-term memory. Learn Mem. 19:319–324.

Lee HHC, Bernard C, Ye Z, Acampora D, Simeone A, Prochiantz A, Di Nardo AA, Hensch TK. 2017. Genetic Otx2 mis-localization delays critical period plasticity across brain regions. Mol Psychiatry. 6:877.

Lennartsson A, Arner E, Fagiolini M, Saxena A, Andersson R, Takahashi H, Noro Y, Sng J, Sandelin A, Hensch TK, Carninci P. 2015. Remodeling of retrotransposon elements during epigenetic induction of adult visual cortical plasticity by HDAC inhibitors. Epigenetics Chromatin. 8:55.

Li L, Carter J, Gao X, Whitehead J, Tourtellotte WG. 2005. The neuroplasticity-associated arc gene is a direct transcriptional target of early growth response (Egr) transcription factors. Mol Cell Biol. 25:10286–10300.

Ma DK, Jang M-H, Guo JU, Kitabatake Y, Chang M-L, Pow-Anpongkul N, Flavell RA, Lu B, Ming G-L, Song H. 2009. Neuronal activity-induced Gadd45b promotes epigenetic DNA demethylation and adult neurogenesis. Science. 323:1074–1077.

Majdan M, Shatz CJ. 2006. Effects of visual experience on activity-dependent gene regulation in cortex. Nat Neurosci. 9:650–659.

Mansur NR, Meyer-Siegler K, Wurzer JC, Sirover MA. 1993. Cell cycle regulation of the glyceraldehyde-3-phosphate dehydrogenase/uracil DNA glycosylase gene in normal human cells. Nucleic Acids Res. 21:993–998.

Mellén M, Ayata P, Dewell S, Kriaucionis S, Heintz N. 2012. MeCP2 binds to 5hmC enriched within active genes and accessible chromatin in the nervous system. Cell. 151:1417–1430.

Meng X, Wang W, Lu H, He L-J, Chen W, Chao ES, Fiorotto ML, Tang B, Herrera JA, Seymour ML, Neul JL, Pereira FA, Tang J, Xue M, Zoghbi HY. 2016. Manipulations of MeCP2 in glutamatergic neurons highlight their contributions to Rett and other neurological disorders. Elife. 5:185.

Niehrs C, Schäfer A. 2012. Active DNA demethylation by Gadd45 and DNA repair. Trends Cell Biol. 22:220–227.

Nott A, Cho S, Seo J, Tsai L-H. 2015. HDAC2 expression in parvalbumin interneurons regulates synaptic plasticity in the mouse visual cortex. Neuroepigenetics. 1:34–40.

Ooi GT, Brown DR, Suh DS, Tseng LY, Rechler MM. 1993. Cycloheximide stabilizes insulin-like growth factor-binding protein-1 (IGFBP-1) mRNA and inhibits IGFBP-1 transcription in H4-II-E rat hepatoma cells. J Biol Chem. 268:16664–16672.

Prochiantz A, Di Nardo AA. 2015. Homeoprotein Signaling in the Developing and Adult Nervous System. Neuron. 85:911–925.

Putignano E, Lonetti G, Cancedda L, Ratto G, Costa M, Maffei L, Pizzorusso T. 2007. Developmental downregulation of histone posttranslational modifications

regulates visual cortical plasticity. Neuron. 53:747–759.

Rai K, Huggins IJ, James SR, Karpf AR, Jones DA, Cairns BR. 2008. DNA demethylation in zebrafish involves the coupling of a deaminase, a glycosylase, and gadd45. Cell. 135:1201–1212.

Rekaik H, Blaudin de Thé F-X, Fuchs J, Massiani-Beaudoin O, Prochiantz A, Joshi RL. 2015. Engrailed Homeoprotein Protects Mesencephalic Dopaminergic Neurons from Oxidative Stress. Cell Rep. 13:242–250.

Rezsohazy R. 2014. Non-transcriptional interactions of Hox proteins: Inventory, facts, and future directions. Dev Dyn. 243:117–131.

Rezsohazy R, Saurin AJ, Maurel-Zaffran C, Graba Y. 2015. Cellular and molecular insights into Hox protein action. Development. 142:1212–1227.

Sampathkumar C, Wu Y-J, Vadhvani M, Trimbuch T, Eickholt B, Rosenmund C. 2016. Loss of MeCP2 disrupts cell autonomous and autocrine BDNF signaling in mouse glutamatergic neurons. Elife. 5:214.

Shepherd JD, Bear MF. 2011. New views of Arc, a master regulator of synaptic plasticity. Nat Neurosci. 14:279–284.

Spatazza J, Lee HHC, Di Nardo AA, Tibaldi L, Joliot A, Hensch TK, Prochiantz A. 2013. Choroid-plexus-derived Otx2 homeoprotein constrains adult cortical plasticity. Cell Rep. 3:1815–1823.

Stettler O, Joshi RL, Wizenmann A, Reingruber J, Holcman D, Bouillot C, Castagner F, Prochiantz A, Moya KL. 2012. Engrailed homeoprotein recruits the adenosine A1 receptor to potentiate ephrin A5 function in retinal growth cones. Development. 139:215–224.

Sugiyama S, Di Nardo AA, Aizawa S, Matsuo I, Volovitch M, Prochiantz A, Hensch TK. 2008. Experience-dependent transfer of Otx2 homeoprotein into the visual

cortex activates postnatal plasticity. Cell. 134:508–520.

Sultan FA, Wang J, Tront J, Liebermann DA, Sweatt JD. 2012. Genetic deletion of Gadd45b, a regulator of active DNA demethylation, enhances long-term memory and synaptic plasticity. Journal of Neuroscience. 32:17059–17066.

Takesian AE, Hensch TK. 2013. Balancing plasticity/stability across brain development. Prog Brain Res. 207:3–34.

Tognini P, Napoli D, Tola J, Silingardi D, Ragione Della F, D'Esposito M, Pizzorusso T. 2015. Experience-dependent DNA methylation regulates plasticity in the developing visual cortex. Nat Neurosci. 18:956–958.

Vallès A, Boender AJ, Gijsbers S, Haast RAM, Martens GJM, de Weerd P. 2011. Genomewide analysis of rat barrel cortex reveals time- and layer-specific mRNA expression changes related to experience-dependent plasticity. Journal of Neuroscience. 31:6140–6158.

Wizenmann A, Brunet I, Lam JSY, Sonnier L, Beurdeley M, Zarbalis K, Weisenhorn-Vogt D, Weinl C, Dwivedy A, Joliot A, Wurst W, Holt C, Prochiantz A. 2009. Extracellular Engrailed participates in the topographic guidance of retinal axons in vivo. Neuron. 64:355–366.

Yokoo T, Knight BW, Sirovich L. 2001. An optimization approach to signal extraction from noisy multivariate data. Neuroimage. 14:1309–1326.

Figure captions

Figure 1. Gadd45b/g are direct targets of Otx2 in the visual cortex of juvenile mice

(A) Otx2-dependent plasticity-associated genes identified through RNA deep sequencing of visual cortex layer IV from *Otx2*$^{+/+}$ (WT) and *Otx2*$^{+/GFP}$ mice at P30 and P100. Relative reads are normalized by reads for *Otx2*$^{+/GFP}$ mice at P30.

(B) Immunohistochemistry of Gapdh (green) and DAPI (blue) in cortex of juvenile mice after cycloheximide (CHX) injection. Inset boxes in left-side panels are magnified in panels to the right. Scale bars, 500 µm (left-side panels) and 50 µm (inset panels).

(C) Visual cortex layer IV expression of candidate genes measured by RT-qPCR following 3 d infusion of CHX or CHX with actinomycin D (ActD) from P20 to P23. Values are fold ratios compared with vehicle-infused samples, averaged from four independent experiments. Error bars, ±SEM; *p<0.05, ****p<0.0001 by two-way ANOVA with Bonferroni posthoc test; mice, control n=11, CHX n=10, CHX+ActD n=7.

(D) *Gadd45b*, *Gadd45g* and *Pvr* expression measured by RT-qPCR 6 hours after visual cortex injection of his-Otx2 recombinant protein with or without CHX. Values are averages of fold ratios compared with vehicle-injected samples. Error bars, ±SEM; *p<0.05, **p<0.01, ***p<0.001 by one-way ANOVA with Bonferroni posthoc test; mice, control n=8, his-Otx2 n=4, his-Otx2+CHX n=4.

(E) *Gadd45b* and *Gadd45g* expression as function of age as measured by RT-qPCR. Values are averages of fold ratios compared to P21. Error bars, ±SEM; *p<0.05 by one-way ANOVA with Bonferroni posthoc test; mice, n=4-6 per age group.

(F-G) *In situ* hybridization (F) of *Gadd45b and Gadd45g* combined with DAB staining of *Wisteria floribunda agglutinin* (WFA) to label PNN. Dotted boxes are magnified in the right-side panels. Co-staining was quantified (G) by number of cells measured in a 600x350 µm area covering the supragranular layers of the binocular zone of adult visual cortex. Scale bars, 50 µm; mice, n=7.

Figure 2. Overexpression of Gadd45b/g in visual cortex induces plasticity gene expression in the adult.

(A) *Gadd45b* and *Gadd45g* expression in visual cortex layer IV of *scFvPax6*$^{tg/o}$ and *scFvOtx2*$^{tg/o}$ adult mice 2 weeks after intraventricular Cre-TAT protein injection. Error bars, ±SEM; *p<0.05 by Student t-test; two independent experiments; mice, *scFvPax6*$^{tg/o}$ n=6, *scFvOtx2*$^{tg/o}$ n=5.

(B) Immunohistochemistry of mCherry (red), PV (green), WFA (grey) in visual cortex of adult mice injected with AAV8-Syn-mCherry-2A-Gadd45b. Scale bar, 200 µm.

(C) Expression of plasticity genes measured by RT-qPCR following viral overexpression of *Gadd45b* in adult mouse visual cortex. Values are averages of fold ratios compared to control (AAV8-Syn-mCherry). Error bars, ±SEM; *p<0.05, **p<0.01 by Student t-test; mice, n=4.

(D) Correlation between expression levels of *Gadd45b* and plasticity genes shown in (C).

Figure 3. Overexpression of Gadd45b in visual cortex reopens the OD plasticity in the adult.

(A-C) Optical imaging maps of responses to the ipsilateral (I) and contralateral (C) eye in the binocular region of V1 in adult wild-type (WT) mice, either (A) un-injected, (B) injected with AAV8-Syn-mCherry, and (C) injected with AAV8-Syn-mCherry-2A-Gadd45b. Monocular deprivation (MD) was performed two weeks after virus injection. Stimulated contralateral and ipsilateral eyes are indicated with a white (open) or black (closed) circle. Top left and middle panels represent the signal magnitude for the retinotopic maps ($\Delta R/R$, $x10^{-4}$) for each eye; bottom left and middle panels indicate corresponding map regularity. Top right panel shows the normalized ocular dominance (OD) map, and bottom right panel shows the OD histogram, with average value inset. Scale bars, 1 mm.

(D) Average OD indices determined in WT mice without MD and virus-injected mice after 4 d of MD. Error bars, ±SEM; *$p<0.05$, **$p<0.01$ by one-way ANOVA with Bonferroni posthoc test; mice, n=6-7 for each group.

(E) Average V1-activation corresponding to values in (D). Error bars, ±SEM; *$p<0.05$, **$p<0.01$ by two-way ANOVA with Bonferroni posthoc test; mice, n=6-7 for each group.

Figure 4. Gadd45b affects the epigenetic state of PNN-enwrapped neurons of the visual cortex.

(A) Immunohistochemistry (IHC) of MeCP2 (green) and WFA (red) in visual cortex layer IV of WT mice at P30 and P100. Scale bar, 10 µm.

(B) Average number of MeCP2 foci in WFA-positive and WFA-negative cells during postnatal development in visual cortex layer IV. Error bars, ±SEM; *p<0.05 by one-way ANOVA with Bonferroni posthoc test; mice, n=6-7 per age group.

(C-D) Distribution of MeCP2 foci area (C) and intensity (D) in WT mice at P30 (grey) and P100 (white). Error bars, ±SEM; mice, n=4 for each age.

(E) Average number of MeCP2 foci in WFA-positive cells in *scFvPax6*$^{tg/o}$ and *scFvOtx2*$^{tg/o}$ mice measured by IHC 2 weeks after intraventricular Cre-TAT protein injection. Error bars, ±SEM; *p<0.05 by Student t-test; mice, n=3 for each genotype.

(F) Average number of MeCP2 foci in WFA-positive cells measured by IHC 2 weeks after viral injection of AAV8-Syn-mCherry or AAV8-Syn-mCherry-2A-Gadd45b in adult visual cortex. Error bars, ±SEM; ***p<0.001 by Student t-test; mice, n=3 for each group.

Figure 1

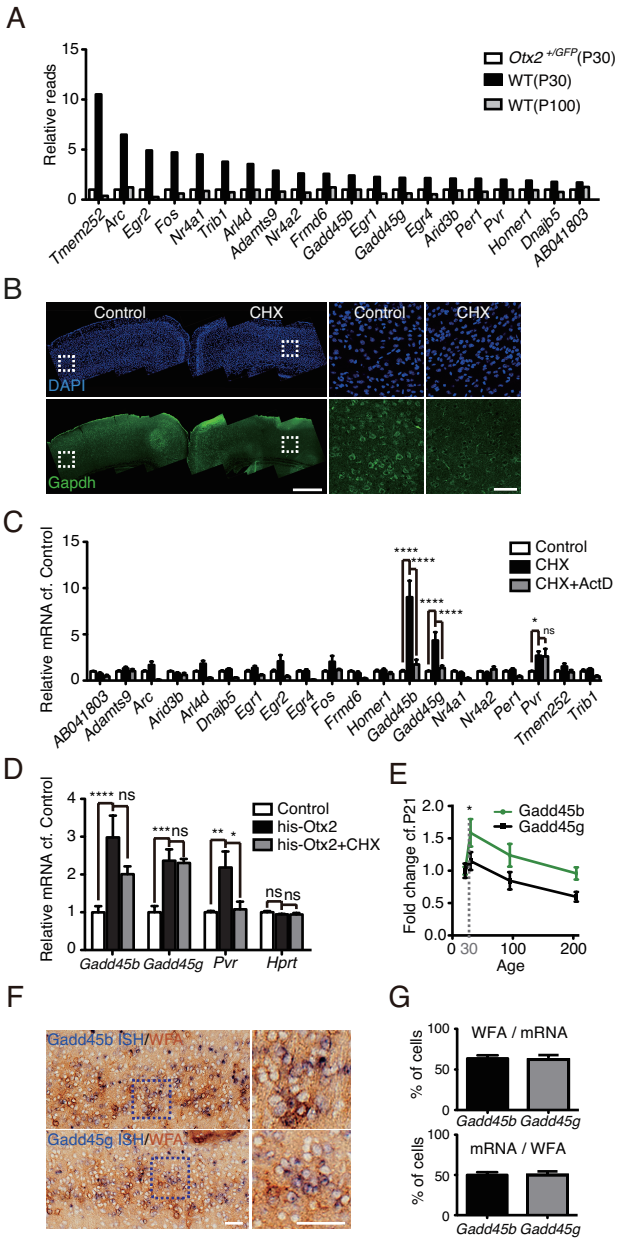
A
Relative reads
Otx2 +/GFP(P30)
WT(P30)
WT(P100)
Tmem252
Arc
Egr2
Fos
Nr4a1
Trib1
Arl4d
Adamts9
Nr4a2
Frmd6
Gadd45b
Egr1
Gadd45g
Egr4
Arid3b
Per1
Pvr
Homer1
Dnajb5
AB041803
B
Control
CHX
DAPI
Gapdh
C
Relative mRNA cf. Control
Control
CHX
CHX+ActD
D
Relative mRNA cf. Control
Control
his-Otx2
his-Otx2+CHX
Gadd45b
Gadd45g
Pvr
Hprt
E
Fold change cf.P21
Gadd45b
Gadd45g
Age
F
Gadd45b ISH/WFA
Gadd45g ISH/WFA
G
% of cells
WFA / mRNA
mRNA / WFA
Gadd45b
Gadd45g

Figure 2

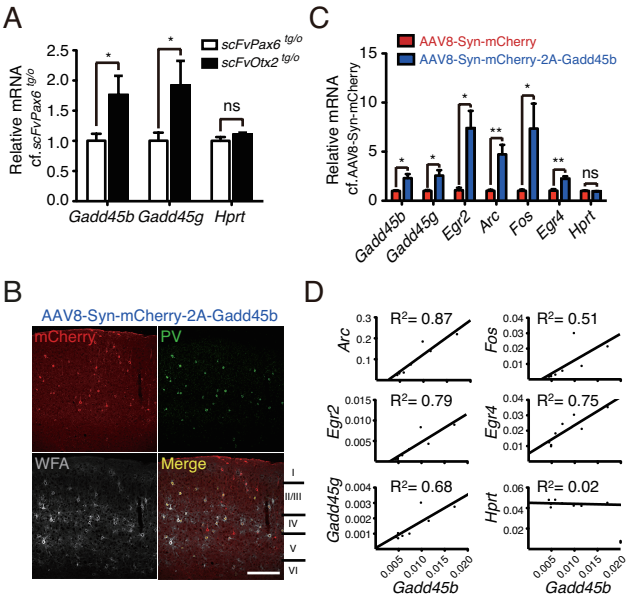
A
Relative mRNA cf. scFvPax6 tg/o
scFvPax6 tg/o
scFvOtx2 tg/o
ns
Gadd45b Gadd45g Hprt
B
AAV8-Syn-mCherry-2A-Gadd45b
mCherry
PV
WFA
Merge
I
II/III
IV
V
VI
C
AAV8-Syn-mCherry
AAV8-Syn-mCherry-2A-Gadd45b
Relative mRNA cf. AAV8-Syn-mCherry
Gadd45b Gadd45g Egr2 Arc Fos Egr4 Hprt
D
Arc R²= 0.87
Fos R²= 0.51
Egr2 R²= 0.79
Egr4 R²= 0.75
Gadd45g R²= 0.68
Hprt R²= 0.02
Gadd45b

Figure 3

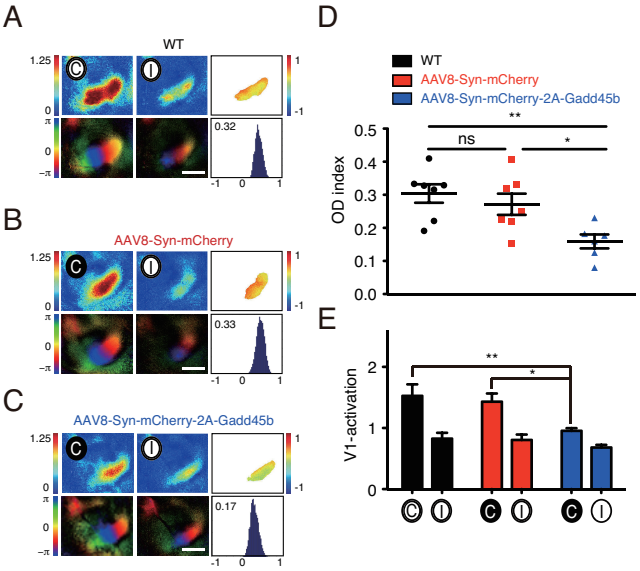
A
WT
1.25
0
π
0
−π
C
I
1
-1
0.32
-1
0
1
B
AAV8-Syn-mCherry
0.33
C
AAV8-Syn-mCherry-2A-Gadd45b
0.17
D
WT
AAV8-Syn-mCherry
AAV8-Syn-mCherry-2A-Gadd45b
OD index
0.5
0.4
0.3
0.2
0.1
0.0
ns
**
*
E
V1-activation
2
1
0
C I C I C I

Figure 4

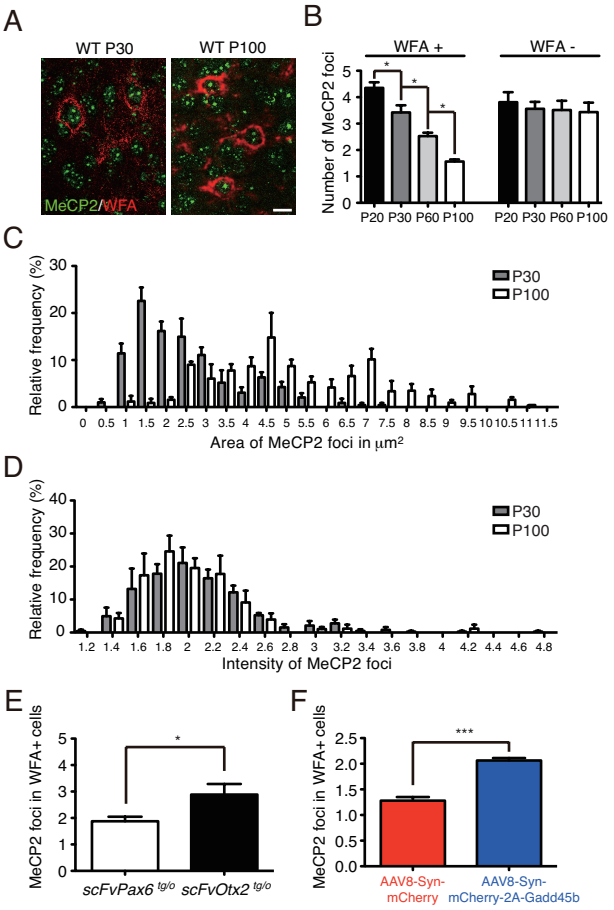
A
WT P30
WT P100
MeCP2/WFA
B
WFA +
WFA -
Number of MeCP2 foci
P20 P30 P60 P100
P20 P30 P60 P100
C
Relative frequency (%)
P30
P100
Area of MeCP2 foci in μm²
D
Relative frequency (%)
P30
P100
Intensity of MeCP2 foci
E
MeCP2 foci in WFA+ cells
scFvPax6 tg/o
scFvOtx2 tg/o
F
MeCP2 foci in WFA+ cells
AAV8-Syn-mCherry
AAV8-Syn-mCherry-2A-Gadd45b